

# CHARACTERIZATION OF GLUTARALDEHYDE COMPOSITION ON PVA-ENZYME COATED PVC-KTPCLPB MEMBRANE WITH XRD, UV-VIS, SEM-EDS, AND FTIR

S. Abd. Hakim<sup>✉</sup>, Satria Mihardi and Abdul Rais

Physics Department, Faculty of Mathematics and Natural Sciences, Universitas Negeri Medan, Medan 20221, Indonesia

<sup>✉</sup>Corresponding Author: [abdhakims@unimed.ac.id](mailto:abdhakims@unimed.ac.id)

## ABSTRACT

An indicator electrode has been made in two ways using the urease enzyme immobilization technique with Glutaraldehyde (GA) crosslinking at various concentrations (2.6 - 3.0)%. The aim is to choose the best indicator electrode from both methods, this is through XRD, SEM-EDS, and FTIR analysis. The method used is a potentiometric biosensor method. The indicator electrode for the first method is denoted PVA-E-GA/PVC-KTpCIPB, meaning that PVA-E is mixed with PVA-E solution coated with PVC-KTpCIPB. The indicator electrode of the second method is denoted PVA-E/GA/PVC-KTpCIPB, meaning that PVA-E coated with GA is coated with PVC-KTpCIPB. Each in 1x, 2x, and 3x layer variations. The best results of GA crosslinking from the first and second methods were at a concentration of 2.9%. The best result of the first method of indicator electrode is PVA-E-GA3x/PVC-KTpCIPB1x. the best result of the second method is the indicator electrode PVA-E 1x/GA 1x/PVC-KTpCIPB 1x.

**Keywords:** Indicator Electrode, Immobilization, XRD, SEM-EDS, and FTIR Analysis.

RASAYAN *J. Chem.*, Vol. 15, No. 4, 2022

## INTRODUCTION

Enzyme immobilization is the process of physical localization of enzymes on certain surfaces which helps to improve some of the properties of enzymes and their operational performance without disturbing their catalytic activity, thereby enabling the recovery and reuse of enzymes so that the whole process can be controlled and economical.<sup>1</sup> Research on indicator electrodes as urea sensors has been carried out using a biosensor potentiometric method with urease enzyme immobilization technique on PVA membrane, namely PVA-Enzyme coated with PVC-KTpCIPB labeled PVA-E-1-2x with Ar notation. 0.0350 g of PVA dissolved in 10 mL of warm water is denoted PVA-E. 0.0350 g PVC-0.0500 g KTpCIPB dissolved in 10 mL THF denoted PVC-KTpCIPB. It has obtained a sensitivity of 19,069 mV/decade, a detection range of  $1.10^{-5} - 5.10^{-4}$  M, a detection limit of  $1.10^{-5}$  M, and a correlation coefficient of 0.9431.<sup>2</sup> Based on the analysis, this detection range is small about the width of the peak absorbance spectrum concerning wavelength. Researchers want to analyze the interaction in the form of molecular adsorption to increase the detection limit and selectivity of the biosensor.<sup>3</sup> Increasing or decreasing glutaraldehyde concentration from 3% causes a decrease in activity,<sup>4</sup> and the optimal glutaraldehyde concentration of 2.5-3% is used for urease immobilization. The techniques used are absorption, trapping, and cross-linking. The cross-linking technique<sup>5</sup> contributes to strengthening the biocatalyst bond, preventing leakage, reducing desorption, and increasing the stability of the biocatalyst. Based on these contributions, the authors chose glutaraldehyde to strengthen the detection range of the urea sensor with an indicator electrode made of tungsten immobilized by the urease enzyme on the indicator electrode. Immobilization of urease enzyme in PVA solution is denoted by PVA-E. There are two cross-links in PVA-E by (1) mixing GA with PVA-E-GA notation and (2) coating PVA-E with GA on the indicator electrode with PVA-E/GA notation. Each of the first and second methods was coated again with PVC-KTpCIPB. The design of the indicator electrode in the first method is denoted PVA-E-GA/PVC-KTpCIPB. The design of the second method is denoted by PVA-E/GA/PVC-KTpCIPB. This aims to obtain the best way to immobilize the urease enzyme. The success of enzyme immobilization and surface modification was measured using a UV-Visible spectrophotometer.<sup>6</sup> The immobilization strategy was then applied to the biosensor application for urea detection.

## EXPERIMENTAL

### Material and Methods

The materials used in this study were the enzyme Uriase, EC 3.5.1.5 (Urea) U4002, 50-100 ix Sigma-Aldrich type, PVA:PVC 1:1 with a mass of 0.0350 g, GA with variations (0.26, 0, 27, 0.28, 0.29, and 0.30) g in 10 mL solvent, KTpCIPB 0.0500 g. This material is used in the form of a solution, the manufacture of indicator electrodes from potentiometer cells using the biosensor potentiometric method modified PVA-E indicator electrode layer crosslinked GA and PVC-KTpCIPB. Crosslinks are modified in two ways. The equipment used in the Physics Laboratory is XRD-6100 Shimadzu, UV-Vis Leigh UV-1601, SEM Evo MA 10 Zeiss, Coating from SEM Q150RES Quorum, Stirrer, and FTIR from the Medan Customs and Excise Laboratory.

### General Procedure

PVA 0.0350 g dissolved in 10 mL of hot water until cold. The urease enzyme 1 mg is dissolved in 0.5 mL of water mixed with alcohol in a ratio of 50%: 50%. Add one drop of the enzyme, and stirred with a Stirrer until mixed into 10 mL cold 0.0350 g PVA. THF was mixed with 0.0350 g PVC and 0.0500 g KTpCIPB in 10 mL. The indicator electrode is made in two ways. In the first method, Glutaraldehyde is mixed with PVA-E to become PVA-E-GA/PVC-KTpCIPB denoted A. The indicator electrode for the second method is PVA-E coated with GA coated again with PVC-KTpCIPB labeled PVA-E/GA/PVC-KTpCIPB denoted B. The method is to obtain the best method in the manufacture of indicator electrodes. The composition of the polymer membrane on the ion selective electrode (ISE) according to<sup>7</sup> by weight 1% ionophore, PVC polymer matrix: plasticizer (1: 2). Synthesis of polymers in the development of ISE sensors according to<sup>8</sup>, membranes at the ratio of Ionophores: PVC: KTCIPB: Plasticizers 10: 165: 5: 330. An increase or decrease in the concentration of glutaraldehyde by more than 3% causes a decrease in activity, determining the optimal concentration of glutaraldehyde between 2.5% -3% for urease enzyme immobilization.

### Detection Method

The first method, fifteen PVA-E-GA 1x/PVC-KTpCIPB 1x indicator electrodes with GA variations (2.6%, 2.7%, 2.8%, 2.9% and 3%) are notated A1-1, A1-2, A1-3, A1-4, and A1-5. Five indicator electrodes PVA-E-GA 2x/PVC-KTpCIPB 1x are denoted A2-1, A2-2, A2-3, A2-4, and A2-5. Five indicator electrodes PVA-E-GA 3x/PVC-KTpCIPB 1x are denoted A3-1, A3-2, A3-3, A3-4, and A3-5. The second method uses the old and new PVC-KTpCIPB. Five indicator electrodes PVA-E1x/GA1x/PVC-KTpCIPB1x with variations in GA (2.6%, 2.7%, 2.8%, 2.9%, and 3%), where PVC-KTpCIPB-old is denoted B1-1-O, B1-2-O, B1-3-O, B1-4-O, and B1-5-O. Five indicator electrodes PVA-E1x/GA1x/PVC-KTpCIPB1x with variations in GA (2.6%, 2.7%, 2.8%, 2.9%, and 3%), where PVC-KTpCIPB-newly denoted B1-1-N, B1-2-N, B1-3-N, B1-4-N, and B1-5-N. All indicator electrodes analyzed by XRD can be seen in Table-1, after being selected, it can be seen in Fig.-1.

### Analytical Discussion

For selecting the best sample, the first step is XRD analysis, the second is UV-Vis analysis, the third is SEM-EDS and the fourth is FTIR. XRD analysis of selected samples with an intensity greater than 200 a, u concerning the diffraction angle of 2theta. Performed for all samples A1, A2, A3, A4, A5; B1-O, B2-O, B3-O, B4-O, and B5-O; B1-N, B2-N, B3-N, B4-N, and B5-N. After selecting the best sample from Table-3 and Fig.-3, the SEM-EDS analysis continued with the selected samples A3-4-O and B1-4-O as shown in Fig.-5a and 5b as the third step. In the second step, only the PVA-E-GA solution was analyzed by UV-Vis from the PVA-GA-E solution, the results can be seen in Fig.-4. The four membranes (a) B1-4-N, (b) B1-4-O, and (c) A3-4-O were analyzed by FTIR see Fig.-6. The final decision in selecting the sample was to find the relationship between all XRD, UV-Vis, SEM-EDS, and FTIR analyses.

## RESULTS AND DISCUSSION

Based on Table-1 sample groups A1, A2, and A3 with variations in GA (2.6%, 2.7%, 2.8%, 2.9%, and 3%) and Ar, the height of the intensity peak changes with the angle of 2Theta. The height of the peak intensity concerning the 2Theta angle of each sample can be seen in Table-1. The highest peak intensity of A1-1 is 270 a.u at 44.28 degrees; A1-2 is 146 a.u at 44.36 degrees; A1-3 is 190 a.u at 44.32; A1-4 is 236 a.u at 44.32 degrees; A1-5 is 278 a.u at 44.28 degrees; Ar is 6306 a.u at 44.52 degrees.

Table-1: The Height of the Peak Concerning Angles 2Theta A1, A2, A3, and Ar

2Theta (degrees)	Intensity (a.u)					
	A1-1	A1-2	A1-3	A1-4	A1-5	Ar
44.28	270	102	136	198	278	330
44.32	238	134	190	236	256	452
44.36	242	146	138	176	256	754
44.52	110	46	56	80	130	6306

2Theta (degrees)	Intensity (a.u)					
	A2-1	A2-2	A2-3	A2-4	A2-5	Ar
44.30	128	166	170	212	230	378
44.32	150	184	212	228	220	452
44.52	52	76	88	84	82	6306

2Theta (degrees)	Intensity (a.u)					
	A3-1	A3-2	A3-3	A3-4	A3-5	Ar
44.28	216	162	352	340	278	330
44.32	220	196	338	382	256	452
44.52	86	62	126	118	130	6306

The highest peak intensity of A2-1 was 150 a.u at 44.32 degrees; A2-2 is 184 a.u at 44.32 degrees; A2-3 is 212 a.u at 44.32 degrees; A2-4 is 228 a.u at 44.32 degrees; A2-5 is 230 a.u at 44.30 degrees, Ar is 6306 a.u at 44.52 degrees. The highest peak intensity of the A3-1 was 220 a.u at 44.32 degrees; A3-2 is 196 a.u at 44.32 degrees; A3-3 is 352 a.u at 44.28 degrees; A3-4 is 382 a.u at 44.32 degrees; A3-5 is 278 a.u at 44.28 degrees. Sample selection based on Table-1 data, the height of the intensity peak with the diffraction angle 2theta greater than 200 au was taken as a sample. The samples are (a) A1-1, (b) A1-4, (c) A1-5 (d) A2-3, (e) A2-4, (f) A2-5, (g) A3-1, (h) A3-3 (i) A3-4, (j) A3-5, and (k) Ar can be seen in Fig.-1. Based on the analysis of Fig.-1, the samples were selected again according to groups, obtained in groups A1 and A3. Group A1 is A1-5 and A2-5, and group A3 is A3-4. The highest intensity peak in the composition A3-4 sees Table-2 and Fig.-2. Analysis of the intensity diffraction spectrum pattern against the 2Theta angle according to<sup>9</sup> shows the diffraction peak at the Bragg angle. Table-2 and Fig.-2 show that the A4 sample group, namely A3-4, has a higher intensity peak than the A5 sample group, namely A1-5. The intensity spectrum pattern against the 2Theta angle of the sample groups A4 and A5 can change the diffraction intensity of Ar. The amorphous spectral patterns in Fig.-1 and 2 are compared with the Ar samples after the addition of GA.

PVA-E mixed with GA labeled PVA-E-GA is the first method of making indicator electrode membranes. Based on Fig.-2, the intensity spectrum pattern concerning angle 2theta, Ar is 6306 a.u at 44.52 degrees, while A3-4 decreases the peak intensity concerning angle 2theta to 382 a.u at 44.32 degrees, due to the addition of 2.9% GA. The optimum concentration of glutaraldehyde in GA is 2.5%.<sup>10</sup> The effect of GA on the biosensor response for a low concentration of 1.5% makes the substrate easy to leak from the membrane due to less cross-linking. For concentrations as high as 3.5%, the biosensor response is less due to more cross-linking, which prevents the substrate from passing through the membrane. Glutaraldehyde cross-linking produces large enzyme aggregates that can serve as catalysts and support for many substrate molecules. Enzyme crosslinking is detrimental to enzyme leaching and the entrapment followed by crosslinking disrupts total binding activity and also greatly enhances enzyme stability in extreme chemical environments.<sup>11</sup> Appropriate addition of glutaraldehyde to produce higher enzyme stability at a concentration of 0.03% glutaraldehyde, in 0.1 M phosphate buffer with a pH variation of 4.5; 5.0; 5.5; 6.0; 6.5; 7.0; 7.5, and 8.0 for 30 minutes.<sup>12</sup> Changes in the height of the peak intensity concerning the 2Theta angle can occur due to the addition of material in PVA. Several results of previous studies (1) PVA-doped

ZnO composites were at an angle of 2theta 30-40 degrees<sup>13</sup>; (2) PVA/SiO<sub>2</sub>-TiO<sub>2</sub> around 2theta 20 degrees<sup>14</sup>; (3) CA and PVA doped ZnO composite nanostructures between 2theta angles of 40-50 degrees<sup>15</sup>; (4) PVA nanofiber hybrids are between 2theta angles of 30-40 degrees<sup>16</sup>; (5) PVA/PAA/Fe<sub>3</sub>O<sub>4</sub> between 2theta angles of 15-20 degrees<sup>17</sup>; (6) The hydroxyapatite-gelatin (HAp-GEL) composite was crosslinked with different GA between 2theta angles of 25-55 degrees.<sup>18</sup>

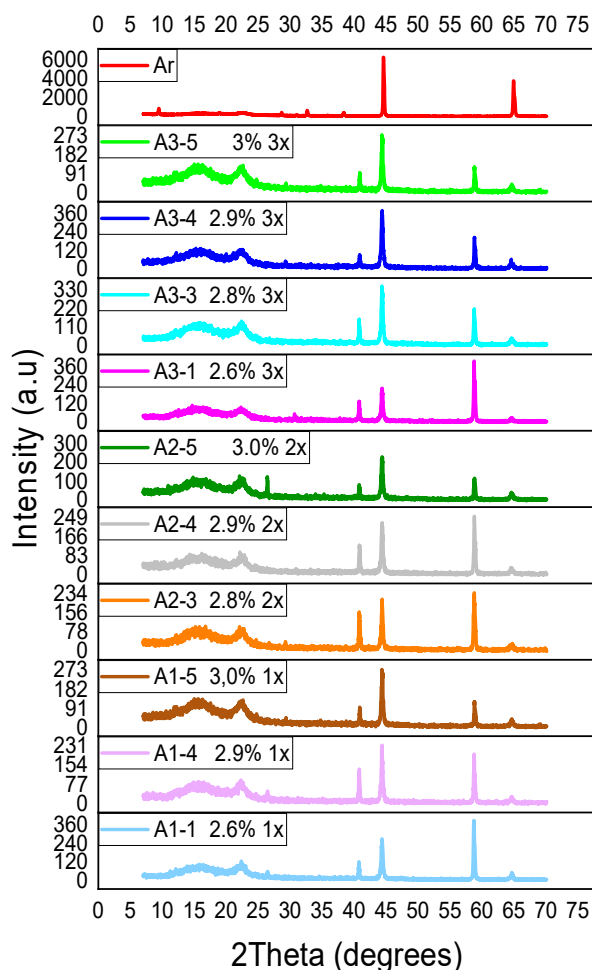


Fig.-1: XRD Diffraction Spectrum Pattern (a) A1-1, (b) A1-4, (c) A1-5 (d) A2-3, (e) A2-4, (f) A2-5, (g) A3-1, (h) A3-3 (i) A3-4, (j) A3-5, and (k) Ar

Table-2: The Highest Intensity Peak Concerning the 2 Theta angle of A1-5; A2-5, A3-4, and Ar

2Theta (degrees)	Intensity (a.u)		2Theta (degrees)	Intensity (a.u)		2Theta (degrees)	Intensity (a.u)	
	A1-5 3,0% 1x	Ar		A2-5 3,0% 1x	Ar		A3-4 3,0% 1x	Ar
44.28	278	330	44.30	230	378	44.28	340	330
44.32	256	452	44.32	220	452	44.32	382	452
44.52	130	6306	44.52	82	6306	44.52	118	6306

When compared with the indicator electrode (Ar), namely PVA-E-1-2x which is coated with PVA-enzyme 1x coated with PVC-KTpCIPB 2x. The 1x PVC-KTpCIPB coated PVA-E-GA coated indicator electrode (1x, 2x, 3x) does not undergo a 2 theta angular shift on a non-decimal scale of approximately 44 degrees.

The method of making the electrode is the first method. The following is the second method for the PVA-enzyme coated indicator electrodes with 2.9% GA coated again with PVC-KTpCIPB (1x, 2x, 3x), with the old PVC-KTpCIPB material with the notation B-4-O and the new PVC-KTpCIPB with the notation B-4-N. GA coated with PVA-E coated again with the old PVC-KTpCIPB coded B1-4-O.

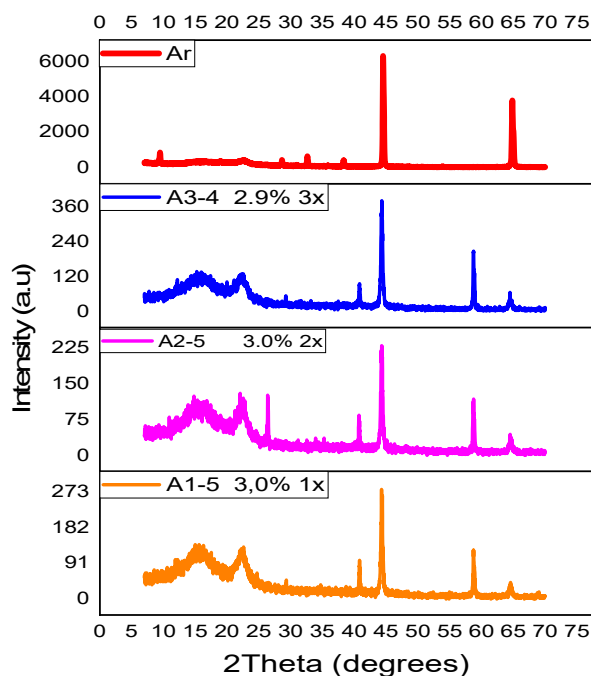


Fig.-2: XRD Diffraction Spectrum Pattern (a) A1-5, (b) A2-5, (c) A3-3 (d) A3-4 and (G) Ar

The indicator electrode was coated with PVA-E coated GA coated again with a new PVC-KTpCIPB with the notation B1-4-N. The intensity of the diffraction spectrum pattern concerning the 2θ angle in a second way from B1-4-O, B2-4-O, B3-4-O (old sample), B1-4-N, B2-4-N, B3-4-N (a new sample) and Ar can be seen in Table-3 and Fig.-3. There is a difference in the intensity spectrum pattern with a 2θ angle. The selected B1-4-O samples peaked above 200 a.u. The highest peak intensity of B1-4-O is 452 a.u at 44.32 degrees. Likewise, the sample B1-4-N was selected for peaks above 200 a.u, the highest peak in the B1-4-N composition was 286 a.u at 44.30 degrees.

Table-3: The Height of the Intensity Peaks Concerning the 2θ Angle of B1-4-O, B2-4-O, B3-4-O; B1-4-N; B2-4-N, A3-4-N, and Ar

2θ (degrees)	Intensity (a.u)			
	B1-4-O	B2-4-O	B3-4-O	Ar
44.30	436	280	278	378
44.32	452	262	280	452
44.34	428	276	286	582
44.52	188	118	116	6.306
2θ (degrees)	Intensity (a.u)			
	B1-4-N	B2-4-N	B3-4-N	Ar
44.30	286	260	127	378
44.52	188	118	116	6.306

Intensity Ar 6306 a.u at an angle of 2θ 44.30 degrees. Analysis of Table-3 and Fig.-3, using the second method, the compositions B1-4-O and B1-4-N were selected, which means that PVA-E coated with GA 1x was further coated with old PVC-KTpCIPB 1x notation B1-O; given the new PVC-KTpCIPB notated as B1-N. This means that PVA-E is coated with 2.9% GA 1x coated again with the old PVC-KTpCIPB 1x with the notation B1-4-O and coated with the new PVC-KTpCIPB 1x with the notation B1-4-N. The two best samples are the second method on the B1-4-O composition, namely the second method of making

indicator electrodes coated with PVA-E 1x coated with 2.9% GA 1x coated again with the old PVC-KTpClPB 1x.

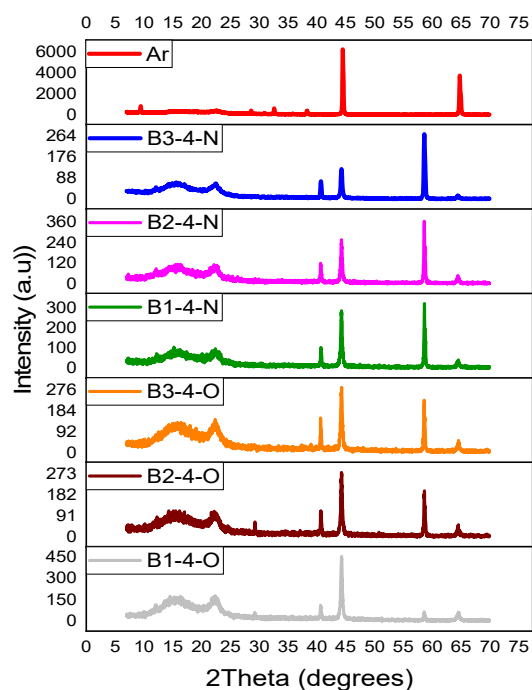


Fig.-3: XRD Diffraction Spectrum Pattern (a) B1-4-O, (b) B2-4-O, (c) B3-4-O (d) B1-4-N, (e) B2-4-N, (f) A3-4-N and (g) Ar

Table-4: Absorbance for PVA-GA-E and PVA-E Solution Wavelengths

Wavelength (nm)	Absorbance (a.u)			
	A1	A4	A5	Ar
291	0.571	0.901	0.732	7.246
299	1.083	1.540	1.370	0.23

After analyzing the method of making indicator electrodes with XRD, the next step is the explanation of the second method using UV-Vis, FTIR, and SEM-EDS analysis. Based on the analysis of UV-Vis analysis, the GA concentration test was carried out between 2.6-3.0% variations in samples A1, A2, A3, A4, and A5 as shown in Table-4 and Fig.-4, the shape is symmetrical.<sup>19,20</sup> There are three samples A1, A4, and A5 whose absorbance spectrum pattern is above 1.000 a.u with wavelengths ranging from 250-400 nm from the PVA-E-GA solution. Based on Fig.-4 (a) the absorption spectrum pattern of Ar has a high absorption peak of 7.246 a.u at a wavelength of 291 nm, while with variations (A) A1; (B) A4; and (C) A5 absorption peak height, respectively 1.083 a.u; 1.540 a.u; 1.370 a.u at a wavelength of about 299 nm. This wavelength shift occurs with the addition of glutaraldehyde. Fig.-4(a), (b), and (c) have a large peak width, while Figure 4 (d) has a small peak width. The UV-Vis absorbance spectrum pattern concerning the wavelength of the PVA-GA-E solution with variations in GA concentration 2.%, 2.9%, and 3.0% formed a symmetrical spectrum pattern (a) A1; (b) A4; and (c) A5 in Fig.-4. The symmetrical pattern of the absorbance spectrum concerning wavelength is supported by.<sup>21</sup> If Fig.-4 (a, b, and c) is compared with the configuration of the PVA-E solution in Fig.-4 (d), then there is a decrease in the absorbance peak height of the solution with variations in the concentration of GA (a) A1; (b) A4; and (c) A5, followed by widening of the absorbance peak see Fig.-4.

Similarly, the determination of the group function in the mixture for the urease enzyme functional group C=O at 1720-1740  $\text{cm}^{-1}$  at B1-4-O absorption frequency 1737.11  $\text{cm}^{-1}$ . PVA coated with GA functional group is O-H at absorption frequency between 3330-3350  $\text{cm}^{-1}$  at B1-4-O absorption frequency 3327.02

$\text{cm}^{-1}$ . A mixture of PVC-KTpCIPB in THF the functional group C-O between  $1100\text{-}1350\text{ cm}^{-1}$  in B1-4-O absorption frequency  $1165.90\text{-}1326.89\text{ cm}^{-1}$  and the acetal ring functional group (C-O-C) between absorption frequency  $1000\text{ - }1140\text{ cm}^{-1}$  in B1-4-O absorption frequency  $1011.06\text{-}1083.60\text{ cm}^{-1}$ .

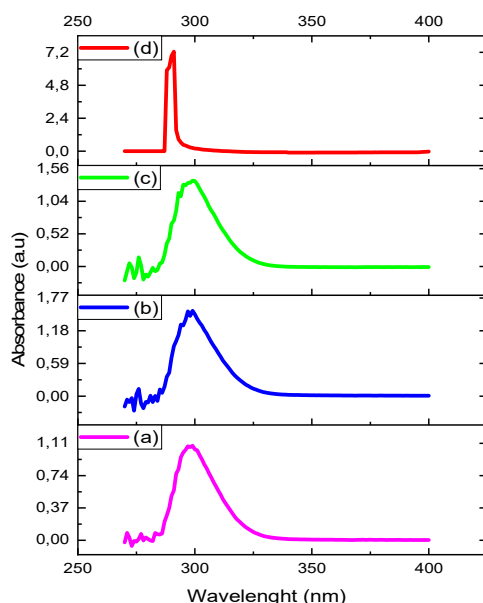


Fig.-4: Pattern of UV-Vis Absorbance Spectrum with Variations in Glutaraldehyde; (a) A1; (b) A4; (c) A5 and (d) Ar

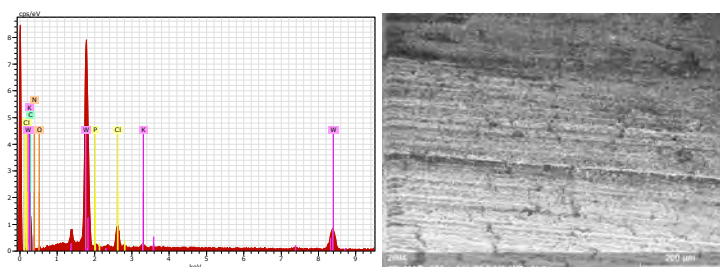


Fig.-5a: EDS Spectrum Pattern and Morphology Indicator Electrode A3-4-O

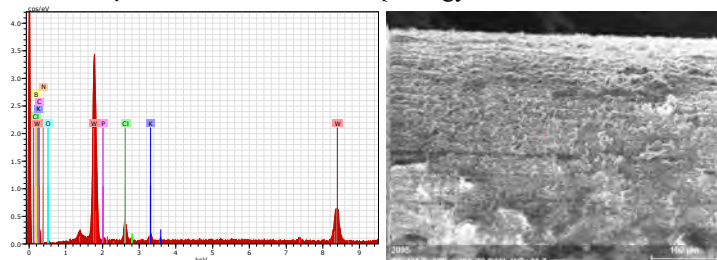


Fig.-5b: EDS Spectrum Pattern and Morphology of Indicator Electrode B1-4-O

The  $\text{Sp}^2$  C-H functional group in the alkene pattern band in the cis group with an absorption frequency of  $675\text{-}730\text{ cm}^{-1}$  and the trisubstituent alkene group with an absorption frequency of  $790\text{-}840\text{ cm}^{-1}$ . In B1-4-O the absorption frequency is  $688.80\text{ cm}^{-1}$  for the cis group with alkene substitution and the absorption frequency is  $798.83\text{ cm}^{-1}$  for the trisubstituent alkene group. Based on Fig.-6 and analysis of spectroscopic table data, there are two C-H hydrogen bands in the aldehyde group with absorption frequencies of  $2800\text{-}2860\text{ cm}^{-1}$  and  $2700\text{-}2760\text{ cm}^{-1}$ . The results were obtained at a B1-4-O absorption frequency of  $2852.16\text{ cm}^{-1}$  and B1-4-N absorption frequency of  $2852.61\text{ cm}^{-1}$  and A3-4-O absorption frequency of  $2832.16\text{ cm}^{-1}$ . Similarly, the determination of the group function in the mixture for the urease enzyme functional group C=O at  $1720\text{-}1740\text{ cm}^{-1}$  at B1-4-O absorption frequency  $1737.11\text{ cm}^{-1}$ . PVA coated with GA functional

group is O–H at absorption frequency between 3330–3350  $\text{cm}^{-1}$  at B1-4-O absorption frequency 3327.02  $\text{cm}^{-1}$ . A mixture of PVC-KTpCIPB in THF the functional group C–O between 1100–1350  $\text{cm}^{-1}$  in B1-4-O absorption frequency 1165.90–1326.89  $\text{cm}^{-1}$  and the acetal ring functional group (C–O–C) between absorption frequency 1000 - 1140  $\text{cm}^{-1}$  in B1-4-O absorption frequency 1011.06–1083.60  $\text{cm}^{-1}$ . The  $\text{Sp}^2$  C–H functional group in the alkene pattern band in the cis group with an absorption frequency of 675–730  $\text{cm}^{-1}$  and the trisubstituted alkene group with an absorption frequency of 790–840  $\text{cm}^{-1}$ . In B1-4-O the absorption frequency is 688.80  $\text{cm}^{-1}$  for the cis group with alkene substitution and the absorption frequency is 798.83  $\text{cm}^{-1}$  for the trisubstituted alkene group.

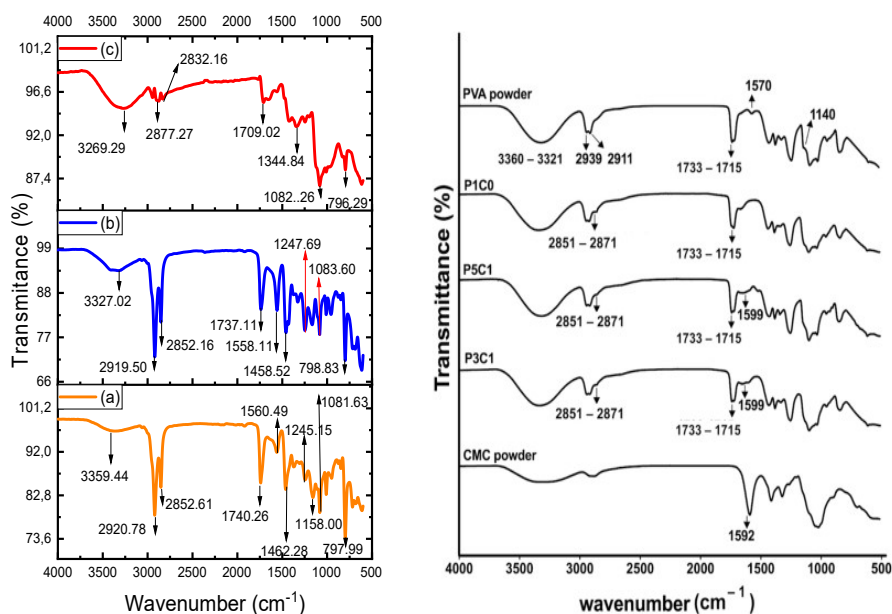


Fig.-6: FTIR Spectrum Pattern of the Sample (a) B1-4-N, (b) B1-4-O, (c) A3-4-O, (d) PVA<sup>27</sup>

According to the FTIR analysis of the pattern of the transmittance spectrum to the wave number, see Fig.-6, it is symmetrical for samples B1-4-N and B1-4-O while samples A3-4-O are not symmetrical. Likewise, XRD analysis in Fig.-3 and SEM-EDS analysis in Fig.-5a and 5b, so that the best sample was selected for the manufacture of indicator electrodes coated with PVA-enzyme 1x coated with 2.9% GA, 1x coated with PVC-KTpCIPB 1x with the notation B1-4. FTIR analysis showed the loss or shift in the absorbance frequency of organic species and functional groups<sup>25</sup> marked by changes in functional groups.<sup>26</sup> FTIR analysis of PVA and GA powders was influenced by the ratio<sup>27</sup> of the FTIR spectral patterns of pure PVA membranes, PVA membranes crosslinked with glutaraldehyde (PVA/GA), and other mixtures.<sup>28</sup> Glutaraldehyde (GA) is a PVA crosslinking agent, substrate characterization of the FTIR spectrum pattern and XRD spectrum pattern showed the relationship between functional groups and crystal properties (metal) with the highest intensity.<sup>29</sup> This is similar to the analysis of the EDS spectrum pattern and the FTIR spectrum pattern.<sup>30</sup> Based on the structural analysis of the EDS spectrum pattern, it was found that the elements K, Cl, O, C, P, B, and tungsten contained in the indicator electrode were supported by the C–H, C=O, O–H, and C–O–C functions.

## CONCLUSION

Based on the description above and analysis in two ways, the conclusions are obtained, the best results are as follows (1): The first method is PVA-enzyme mixed with 2.9% GA with the notation PVA-E-GA, the indicator electrode is coated with PVA-E-GA 3x coated with PVC-KTpCIPB 1x, become PVA-E-GA3x/PVC-KTpCIPB1x with the notation A3-4-O; (2) the second method is PVA-enzyme coated with 2.9% GA with the notation PVA-E/GA, the indicator electrode is coated with PVA-E 1x coated with GA 1x again coated with PVC-KTpCIPB 1x, becoming PVA-E 1x/GA 1x/PVC-KTpCIPB 1x, denoted B1-4-N. There is an analytical relationship between XRD, SEM-EDS, and FTIR in selecting samples for making indicator electrodes using the urease enzyme immobilization technique.

## ACKNOWLEDGEMENT

The author would like to thank the Chancellor of the State University of Medan who has provided research grants for BASIC RESEARCH, the Chairman of the Research and Community Service Institute Universitas Negeri Medan, the Physics Laboratory of the Universitas Negeri Medan, and LIPI-Bandung.

## REFERENCES

1. A. N. Singh, S. Singh, V. K. Dubey, PLoS ONE, **8(6)**, e66000(2013), <https://doi.org/10.1371/journal.pone.0066000>
2. A. Hakim S., T. Sembiring, K. Tarigan, K. Sebayang, M. Situmorang and N. M. Noer, *Rasayan Journal of Chemistry*, **12(2)**, 780(2019), <https://doi.org/10.31788/rjc.2019.1225143>
3. G. Ma, S. Zhao, J. Jiang, H. Song, C. Li, Y. Luo, and H. Wu, *Scientific Reports*, **7**, Article number: 14961(2017), <https://doi.org/10.1038/s41598-017-13823-0>
4. A. M. Kayastha, and P. K. Srivastava, *Applied Biochemistry and Biotechnology*, **96**,41(2001), <https://doi.org/10.1385/abab:96:1-3:041>
5. A. A. Ismaiel, M. K. Aroua, R. Yusoff, *International Journal of Environmental Science and Technology*, **11**,1115(2014), <https://doi.org/10.1007/s13762-013-0296-y>
6. W. E. F. W. Khalid, L. Y. Heng and M. N. M. Arip, *Sains Malaysiana*, **47(5)**, 941(2018), <https://doi.org/10.17576/jsm-2018-4705-09>
7. L. Górski, D. Klimaszewska, M. Pietrzak and E. Malinowska, *Analytical and Bioanalytical Chemistry*, **389**, 533(2007)
8. D. Vlascici, E. F. Cosma, E. M. Pica, V. Cosma, O. Bizerea, G. Mihailescu and L. Olenic, *Sensors*, **8**, 4995(2008) <https://doi.org/10.3390/s8084995>
9. N. Sabli, N.A. Abu Bakar, S. Izhar and H.S. Hilal, *Sains Malaysiana*, **48(4)**, 877(2019), <https://doi.org/10.17576/jsm-2019-4804-20>
10. D. Manoj, Ishita Auddy, Shubham Nimbkar, S. Chittibabu, and S. Shanmugasundaram, *Hindawi International Journal of Food Science*, Article ID 1696201, 7 pages, (2020), <https://doi.org/10.1155/2020/1696201>
11. Bharat Bhushan, Ajay Pal, and Veena Jain, *Hindawi Publishing Corporation Enzyme Research*, Article ID 210784, 9 pages, (2015), <https://doi.org/10.1155/2015/210784>
12. Y Witazora, Yandri, T Suhartati, H Satria and S Hadi, *Journal of Physics: Conference Series*,**1751**, 012097, (2021), <https://doi.org/10.1088/1742-6596/1751/1/012097>
13. N. B. Within Kumar, Vincent Crasta, and B. M. Praveen, *Nanoparticles*, Article ID 742378, 9 pages, (2014), <https://doi.org/10.1155/2014/742378>
14. H. Ma, T. Shi and Q. Song, *Fibers*, **2**, 275(2014), <https://doi.org/10.3390/fib2040275>
15. A. N. Mallika, A. Ramachandra Reddy, K. Venugopal Reddy, *Journal of Advanced Ceramics*, **4(2)**, 123(2015) <https://doi.org/10.1007/s40145-015-0142-4>
16. Y. Meng, *Nanomaterials*, **5**, 1124(2015), <https://doi.org/10.3390/nano5021124>
17. Z. Gao, Y. Yi, J. Zhao, Y. Xia, M. Jiang, F. Cao, H. Zhou, P. Wei, H. Jia and X. Yong, *Bioresour. Bioprocess*, **5(27)**, 2(2018), <https://doi.org/10.1186/s40643-018-0215-7>
18. N. E. Aydin, *International Journal of Polymer Science*, Article ID 8017035, 13 pages, (2020), <https://doi.org/10.1155/2020/8017035>
19. A. S. Rini, Y. Rati, M. Agustin, Y. Hamzah and A. A. Umar, *Sains Malaysiana*, **49(12)**, 3055(2020), <https://doi.org/10.17576/jsm-2020-4912-17>
20. J. Qaderi, C. R. Mamat and A. A. Jalil, *Sains Malaysiana*, **50(1)**, 135(2021), <https://doi.org/10.17576/jsm-2021-5001-14>
21. M. Bilal, Y. Zhao, T. Rasheed, I. Ahmed, S.T.S. Hassan, M. Z. Nawaz and H.M.N. Iqbal, *International Journal of Environmental Research and Public Health*, **16**, 598(2019), <https://doi.org/10.3390/ijerph16040598>
22. M. Cruz, K. Fernandes, C. Cysneiros, R. Nassar, and S. Caramori, *Hindawi Publishing Corporation BioMed Research International*, Article ID 145903, 9 pages (2015), <https://doi.org/10.1155/2015/145903>
23. B. H. Musa, N.J. Hameed, *Journal of Physics: Conference Series*, **1795**, 012064(2021),

- <https://doi.org/10.1088/1742-6596/1795/1/012064>
24. A. Care, K. Petroll, E. S. Y. Gibson, P. L. Bergquist, and A. Sunna, *Biotechnology for Biofuels* , **10**, 29(2017), <https://doi.org/10.1186/s13068-017-0715-2>
  25. M. F .MD Nasir, W. R. W. Daud, M. A. Mohamed, M. H. Mamat, S. Abdullah and M. R. Mahmood, *Sains Malaysiana*, **49(12)**, 3219(2020), <https://doi.org/10.17576/jsm-2020-4912-33>
  26. R. Permadi, V. R. Eh Suk and M. Misran, *Sains Malaysiana*, **49(9)**, 2251(2020), <https://doi.org/10.17576/jsm-2020-4909-22>
  27. J. Namkaew, S. Honsawek, P. Laowpanitchakorn, N. Sawaddee, S. Jirajessada, and S. Yodmuang, *Engineering Molecules*, **26**, 578(2021), <https://doi.org/10.3390/molecules26030578>
  28. K. Knozowska, J. Kujawa, R. Lagzdins, A. Figoli, and W. Kujawski, *Materials*, **13**, 3676(2020), <https://doi.org/10.3390/ma13173676>
  29. L. Blanco-Covián, J. R. Campello-García, M. C. Blanco-López and M. Miranda-Martínez, *Applied Science* **10**, 5864(2020), <https://doi.org/10.3390/app10175864>
  30. L. Y. Jun, N. M. Mubarak, L. S. Yon, C. H. Bing, M. Khalid, P. Jagadish and E. C. Abdullah, *Scientific Reports*, **9**, 2215(2019), <https://doi.org/10.1038/s41598-019-39621-4>

[RJC-7073/2022]